

Molecular beam epitaxial growth and characterization of zinc-blende ZnMgSe on InP (001)

Mohammad Sohel, Martin Muñoz,^{a)} and Maria C. Tamargo^{b)}

Department of Chemistry of the City College of New York and Graduate Center of CUNY, New York, New York 10031

(Received 18 May 2004; accepted 11 August 2004)

High crystalline quality zinc-blende structure $\text{Zn}_{(1-x)}\text{Mg}_x\text{Se}$ epitaxial layers were grown on InP (001) substrates by molecular beam epitaxy. Their band gap energies were determined as a function of Mg concentration and a linear dependence was observed. The band gap of the $\text{Zn}_{(1-x)}\text{Mg}_x\text{Se}$ closely lattice matched to InP was found to be 3.59 eV at 77 K and the extrapolated value for zinc-blende MgSe was determined to be 3.74 eV. Quantum wells of $\text{Zn}_{(1-x)}\text{Cd}_x\text{Se}$ with $\text{Zn}_{(1-x)}\text{Mg}_x\text{Se}$ as the barrier layer were grown which exhibit near ultraviolet emission. © 2004 American Institute of Physics. [DOI: 10.1063/1.1804611]

Mg-based II–VI materials are of considerable interest for the fabrication of optoelectronic devices because their band gaps can be controlled as function of Mg concentration, offering a tuning of the optical confinement.¹ In particular, wide band gap $\text{Zn}_{(1-x)}\text{Mg}_x\text{Se}$ has potential application as a cladding layer for optical devices in the blue region due to its wide direct band gap.² The $\text{Zn}_{(1-x)}\text{Mg}_x\text{Se}$ alloys have been grown on GaAs substrates^{3–5} and on InAs substrates.⁶ It has been reported^{5,7} that $\text{Zn}_{(1-x)}\text{Mg}_x\text{Se}$ with more than 40% Mg undergoes a phase transition from zinc blende to rock salt, so that the maximum band gap of the zinc-blende phase layers grown on GaAs reported by these authors is about 3.1 eV. The use of an InP substrate is an alternative to further increase the band gap of zinc-blende $\text{Zn}_{(1-x)}\text{Mg}_x\text{Se}$ up to ~3.62 eV when grown nearly lattice matched to InP, which will make it more attractive as a cladding layer for higher carrier confinement. In this work, we report the MBE growth and characterization of the ternary alloy $\text{Zn}_{(1-x)}\text{Mg}_x\text{Se}$ nearly lattice matched to InP substrates with a band gap ranging from 3.49 to 3.62 eV at 77 K.

A series of $\text{Zn}_{(1-x)}\text{Mg}_x\text{Se}$ epitaxial layers were grown on InP (001) substrates by MBE using a dual chamber Riber 2300P MBE system that includes one chamber for the growth of As-based III–V materials and another for the growth of wide gap II–VI materials, the two connected by ultrahigh vacuum (UHV) transfer modules. Solid source materials Zn, Mg, Se with a purity of 6N were used. Semi-insulating epi-ready InP (001) substrates were used. Oxide desorption of the InP substrate was performed thermally in the III–V chamber by heating to 490 °C under an As flux. Deoxidation of the substrate and growths were monitored *in situ* by reflection high-energy electron diffraction (RHEED). A lattice matched InGaAs buffer layer of ~0.1 μm was grown, exhibiting a streaky (2 × 4) RHEED pattern throughout the growth. The substrate with the buffer layer was transferred to the II–VI chamber via the UHV transfer module. The growth of the epilayers in the II–VI chamber was performed under Se-rich conditions. The VI to II flux ratio was

between 4 and 6. The growth was initiated at 170 °C in the II–VI chamber with a 40 s exposure of the InGaAs (2 × 4) surface to the Zn flux (Zn-irradiation) prior to initiating the growth. This step is useful to avoid any interaction of Se at the III–V/II–VI interface, and it was followed by a growth of ~50 Å of a ZnCdSe “interfacial layer” at 170 °C. Growth was interrupted and the substrate temperature adjusted to the desired growth temperature. At 250 °C an ~80-Å-thick $\text{Zn}_{(1-x)}\text{Mg}_x\text{Se}$ buffer layer was grown. Then a thick (~0.8 μm) $\text{Zn}_{(1-x)}\text{Mg}_x\text{Se}$ epilayer was grown at 270 °C. Several samples were grown with different composition. A streaky (2 × 1) RHEED pattern was observed throughout the growth of the II–VI material, indicating the zinc-blende phase stability and the absence of facet formation. Since high Mg content materials are highly reactive and hygroscopic, the samples were capped with a thin ~50-Å-thick ZnCdSe cap layer to avoid oxidation.

The $\text{Zn}_{(1-x)}\text{Mg}_x\text{Se}$ crystalline quality was assessed by double crystal x-ray diffraction (DCXRD) measurements using a double-crystal biaxial diffractometer and Cu Kα₁ radiation. In order to calculate the bulk lattice constant the (004) symmetrical reflection and the (115) *a* and *b* asymmetrical reflections of the DCXRD rocking curves were obtained. From the (115) *a* and *b* asymmetrical reflections the lattice constant of the epitaxial layer perpendicular and parallel to the growth surface can be obtained.⁸ From the comparison of the perpendicular and parallel lattice constants it was found that the samples were only partially relaxed. These values allow us to calculate the bulk (relaxed) lattice constant of the layers. The compositions of the films were determined using the bulk lattice constant and a linear interpolation between the lattice constants of ZnSe, 5.668 Å,¹ and MgSe, 5.90 Å, the last value is an average of the two reported values,⁶ 5.89 and 5.904 Å, respectively. Photoluminescence (PL) measurements were performed at 77 K using the 325 nm line of the He–Cd laser for excitation. Reflectance measurements were performed using a Cary500 spectrophotometer.

Samples were grown with Mg content from 65% up to lattice-matched conditions (with ~87% Mg) or slightly in excess of Mg (up to 92% Mg). All the samples were found to be of the zinc-blende structure. During the growth of the ZnMgSe epilayers, the RHEED showed streaky (2 × 1) zinc-blende pattern throughout. A very slow growth rate of ~0.4

^{a)}Present address: Physics Department, Virginia Commonwealth University, Richmond, VA; electronic mail: mmunoz@VCU.edu

^{b)}Electronic mail: tamar@sci.cuny.cuny.edu

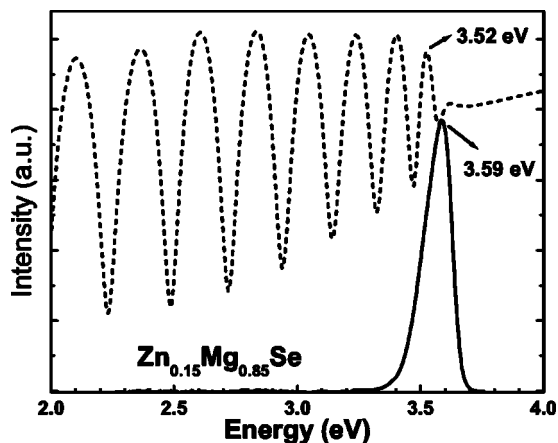


FIG. 1. 77 K PL and room temperature reflectance spectra of a $Zn_{0.15}Mg_{0.85}Se$ epilayer.

to $\sim 0.5 \mu\text{m/h}$ was maintained during the growth as it was observed that too fast a growth in some cases led to the spotty RHEED pattern. Wide-angle analysis ($10^\circ\text{--}70^\circ$) of the single crystal x ray has shown no additional peaks, confirming the absence of rocksalt structure with the higher Mg contents.

Figure 1 shows the PL at 77 K and the room temperature (RT) reflectance spectra of a sample with 85% of Mg (near lattice matched to InP). A very efficient PL emission at 3.59 eV was observed with a full width at half maximum of ~ 103 meV. We observed that the width of the peak increased with increasing Mg content in the alloy. Also, no deep level emission, characteristic of poor material quality, was observed in any of the samples. The RT band gap of the sample from the reflectance measurement was found to be 3.52 eV and differs by 0.07 eV from the PL value, which corresponds to the temperature dependence of the band gap. The PL and reflectance spectra were overlapped in the figure to illustrate the direct band gap origin.

Figure 2 presents the double crystal x-ray rocking curve of a $0.55\text{-}\mu\text{m}$ -thick $Zn_{0.09}Mg_{0.91}Se$ layer with a 0.18% ($\Delta a/a \times 100$) lattice mismatch to the InP substrate. The inset in this figure shows the room temperature reflectance mea-

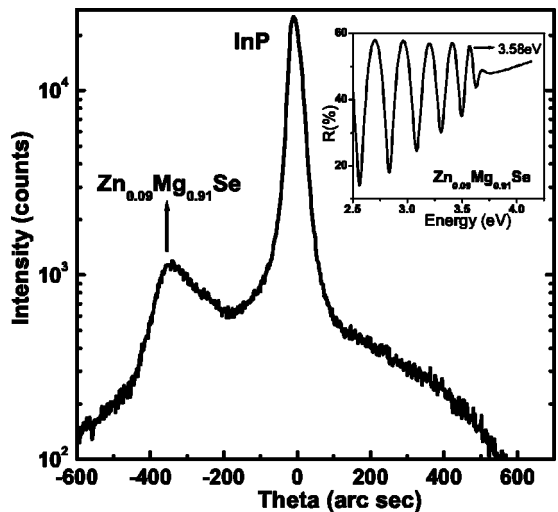


FIG. 2. (a) (004) reflection double crystal x-ray rocking curve spectrum of a $0.55\text{-}\mu\text{m}$ -thick $Zn_{0.09}Mg_{0.91}Se$. (b) Room temperature reflectance measurement of the same sample.

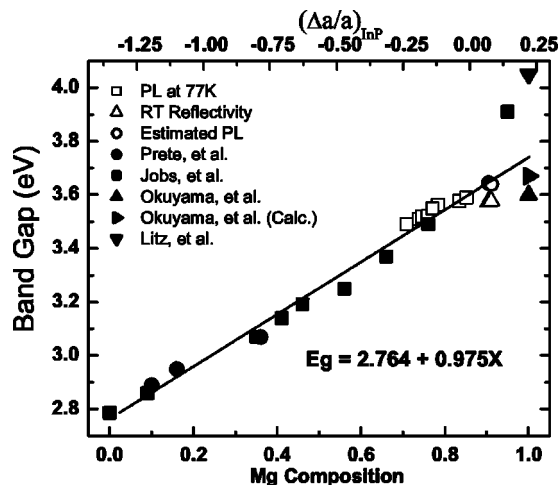


FIG. 3. Band gap energies of $Zn_{1-x}Mg_xSe$ alloys as a function of the Mg concentration and the lattice mismatch to InP. The sources of these data are our PL experiments at 77 K (\square), our reflectance measurements at RT (Δ), estimated band gap at 77 K using our RT measurements (\circ), and Refs. 2,3,6,9 and 11 (\bullet , \blacksquare , \blacktriangle , \blacktriangledown , and \blacktriangleright), respectively.

surement indicating a band gap of 3.58 eV. The PL measurement of this sample is not possible with our experimental setup because of the proximity of this emission to the 325 nm He-Cd laser line. In most of these samples we have observed a very low intensity of the peak of the epilayer in the x-ray measurement. This behavior is consistent with previous reports.⁹ In order to understand this behavior we have estimated the relative intensity of the peaks via the calculation of the structure factor¹⁰ for ZnSe, MgSe, ZnCdSe, and ZnMgSe. The calculated relative intensity of ZnMgSe was found to be very small. This is related to the very small size of the magnesium atom, which exhibits an inefficient x-ray scattering process.

Figure 3 shows the band gap energy as a function of Mg concentration and lattice mismatch to InP substrate of the $Zn_{(1-x)}Mg_xSe$ alloys. The open square data points are taken from our PL measurements at 77 K, the open triangles are from our reflectance measurements at RT, and the open circles are the estimated 77K PL values for the same samples. We have done this estimation because the PL emission of these samples was close to the laser line, and thus could not be directly measured at 77 K. To estimate the 77 K value of the band gap we added 0.07 eV to the band gap value obtained by reflectivity measurements at RT, which is the average observed difference between the PL and reflectivity measurements in the samples for which both measurements were possible. The filled circles, filled squares, and filled up- and side-triangles are the band gap values of $Zn_{(1-x)}Mg_xSe$ alloys grown on GaAs reported in Refs. 2,3,9 and 11, respectively, and the filled inverted-triangle represents the band gap of MgSe grown on InAs, reported by Litz.⁶ A linear relationship between Mg concentration and band gap was observed for our measurements and for most of the reported values, and is in excellent agreement with Vegards law. Lattice matched $Zn_{(1-x)}Mg_xSe$ was grown on InP substrates with a band gap of ~ 3.59 eV with 87% Mg. Furthermore, with higher Mg content the band gap of the ZnMgSe grown on InP substrates was tuned to ~ 3.66 eV. The relationship between band gap (E) and composition (x) at 77 K is given by the following empirical formula: $E(x)$

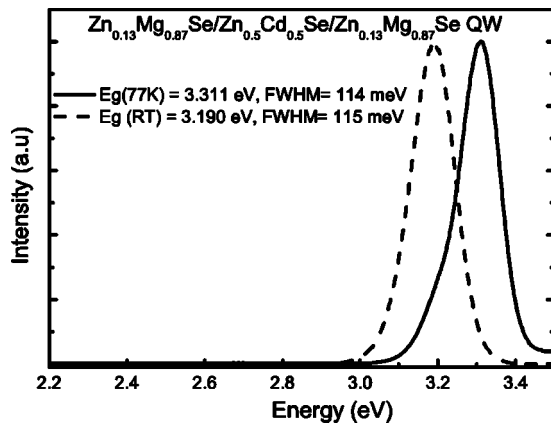


FIG. 4. Near-UV PL emission of a lattice-matched ZnMgSe/ZnCdSe QW structure grown on InP.

$=2.764+0.975x$; where $x(0 \leq x \leq 1)$ is the Mg concentration. Figure 3 shows agreement between the band gap values in the literature and this linear relationship for concentrations of Mg up to 80%. For high Mg concentrations Ref. 7 reported that when $Zn_{(1-x)}Mg_xSe$ is grown on GaAs it undergoes a phase transition from zinc blende to rock salt. References 3 and 6 reported a very large increase in the band gap for samples with 95% and 100% Mg grown on GaAs and on InAs, respectively. However, our measurements clearly indicate that when high crystalline quality, zinc-blende layers are grown the linear relationship holds for values up to 92% Mg. We conclude that the observation of these very large band-gap values by others is due to the fact that these samples were grown with a very large lattice mismatch to the substrate resulting in a very large strain, which as pointed out in Ref. 7, makes it likely that they contain rocksalt phase. The existence of the bowing parameter of the band gap of $Zn_{(1-x)}Mg_xSe$ as function of the Mg composition, reported in Ref. 3, is based on the band gaps of these two anomalous samples. Our results for a large number of samples with compositions between 65% and 95% Mg shows that this bowing is not present. Using an extrapolation based on the linear fit shown in Fig. 3, it follows that the band gap of zinc-blende MgSe is 3.74 eV, which is in close agreement with the calculated values of 3.67 eV¹¹ and the 3.6 eV value reported in Refs. 2 and 11. The linear dependence of the band gap and the Mg concentration presented in this work is in agreement with the first principles calculations of the bowing parameter of Ref. 11 based on Van Vechten's method¹² and those based on Hill's theory,¹³ both of which indicate that this value is zero.

The potential use of a ZnMgSe barrier in device structures is illustrated in Fig. 4, which shows a 6-Å-thick ZnCdSe quantum well (QW) with ZnMgSe barriers, all

lattice-matched to the InP substrate, having a strong PL emission in the near-ultraviolet region. Another potential use of this kind of QW structure is in intersubband devices, i.e., devices that rely on intersubband transitions within a well, because it is expected¹⁴ that approximately 80% of the band gap discontinuity will be in the conduction band, presenting the possibility of quantum cascade lasers operating at shorter wavelengths and with a better thermal performance.

In summary, a series of zinc-blende structure $Zn_{(1-x)}Mg_xSe$ layers were grown by MBE on InP substrates with excellent crystalline quality. Their band gaps were determined by PL and reflectance measurements. The band gap was adjusted up to ~ 3.66 eV with increasing Mg content. A linear dependency was observed between the band gap and the Mg concentration of the ZnMgSe alloys, predicting a value of the band gap for zinc-blende MgSe of 3.74 eV. Wide-angle single crystal x-ray measurements have confirmed the absence of rocksalt phase formation in the ZnMgSe alloys grown on InP. High quality ZnCdSe QW with ZnMgSe barrier layers exhibiting emission in the blue and near-UV regions were grown on InP substrates, suggesting potential uses of these structures in devices.

This work was supported by the National Science Foundation through Grant No. ECS0217646. Partial support was also obtained from the Center for Analysis of Structures and Interfaces, and the New York State Center for Advanced Technology on Photonic Materials and Applications.

¹*II-VI Semiconductor Materials and their Applications*, edited by M. C. Tamargo (Taylor and Francis, New York, 2002).

²H. Okuyama, K. Nakano, T. Miyajima, and K. Akimoto, *Jpn. J. Appl. Phys., Part 2* **30**, L1620 (1991).

³B. Jobst, D. Hommel, U. Luntz, T. Gerhard, and G. Landwehr, *Appl. Phys. Lett.* **69**, 97 (1996).

⁴M. Woz, E. Griebel, Th. Reisinger, R. Flierl, B. Haserer, T. Semmler, T. Frey, and W. Gebhardt, *Phys. Status Solidi B* **202**, 805 (1997).

⁵B. Vögele, C. Morhain, B. Urbaszek, S. A. Telfer, K. A. Prior, and B. C. Cavenett, *J. Cryst. Growth* **201/202**, 950 (1999).

⁶M. Th. Litz, K. Watanabe, M. Korn, H. Röss, U. Luntz, W. Ossau, A. Waag, G. Landwehr, Th. Walter, B. Neubauer, D. Gerthsen, and U. Schüssler, *J. Cryst. Growth* **159**, 54 (1996).

⁷C. Morhain, D. Seghier, B. Vögele, C. O'Donnell, K. A. Prior, B. C. Cavenett, and H. P. Gislason, *J. Cryst. Growth* **214/215**, 482, (2000).

⁸S. P. Guo, X. Zhou, O. Maksimov, and M. C. Tamargo *J. Vac. Sci. Technol. B* **19**, 1635 (2001).

⁹P. Prete, N. Lovergine, L. Tapfer, C. Zanotti-Fregonara, and A. M. Mancini, *J. Cryst. Growth* **214/215**, 119 (2000).

¹⁰B. D. Cullity, *Elements of X-ray Diffraction* (Adison-Wesley, Reading, MA, 1977).

¹¹H. Okuyama, Y. Kishita, and A. Ishibashi, *Phys. Rev. B* **57**, 2257 (1998).

¹²J. A. Van Vechten and T. K. Bergstresser, *Phys. Rev. B* **1**, 3351 (1970).

¹³R. Hill, *J. Phys. C* **7**, 521 (1974).

¹⁴M. Muñoz, H. Lu, X. Zhou, M. C. Tamargo, and F. H. Pollak, *Appl. Phys. Lett.* **83**, 1995 (2003).